SUPERCONDUCTING MAGNET SYSTEM FOR AN EXPERIMENTAL DISK MHD FACILITY

H.G. Knoopers, H.H.J. ten Kate, L.J.M van de Klundert,
P. Massee[+] and W.J.M. Balemans[+].
Applied Superconductivity Centre, University of Twente,
P.O.B. 217, 7500 AE Enschede, The Netherlands, and
(+) Eindhoven University of Technology,
P.O.B. 513, 5600 MB Eindhoven, The Netherlands.

Abstract

In this paper a predesign of a split-pair magnet for an MHD facility for testing a 10 MWt open cycle disk or a 5 MWt closed cycle disk generator is presented. The magnet system consists of a NbTi and a Nb_3Sn section providing a magnetic field of 9 T in the active area of the MHD channel. After discussion of the optimization process which is based on minimum conductor costs, the proposed conductor design is described. Furthermore, basic solutions for the construction of the magnet, the cryostat and the cooling technique are presented.

Introduction

The total efficiency of a coal fired electricity power plant can be improved by using an MHD generator as a topping cycle. In a resently published system study[1] the performance of four large scale (1000 MWt) MHD systems was compared, i.e. the disk and the linear generator both for open cycle and for closed cycle conditions. It was concluded that the closed cycle disk generator has a small advantage over the other three systems when the coal to bus bar efficiency is considered. Furthermore, due to its geometry, the disk generator has additional advantages over the linear generator, as a more simple electrode geometry and a more compact generator configuration leading to lower construction costs mainly due to the less expensive superconducting magnet system.

A conceptual design of an experimental test facility for testing disk shaped generators at high magnetic fields is now completed[2]. An impression of the cryogenic system is shown in figure 1.

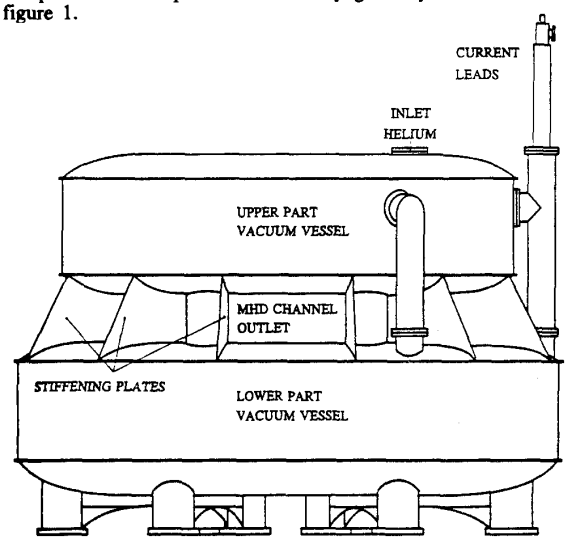

Figure 1. Outside view of the disk MHD cryogenic system.

Generator characteristics

The aim of the proposed disk MHD facility is to continue the study of a generator type with promising advantages but which is less developed than the open cycle linear MHD generator. Both open cycle and closed cycle disk generators can be placed inside the same magnet. A line diagram of the open cycle facility is given in figure 2. To obtain the best results with respect to

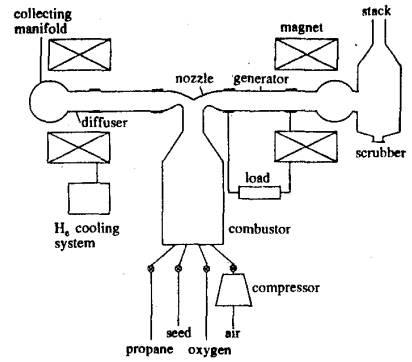

Figure 2. Line diagram of an open cycle disk MHD facility.

enthalpy extraction, calculations are performed in which the following parameters are varied: the Mach number at the channel inlet; the inlet swirl; the pressure of the combustion air and the seed ratio. In table 1 a few important parameters of the optimal disk MHD generators are collected. The reader is referred to ref. 2 for extensive information about the disk generator properties.

Table 1. Parameters of the optimal disk MHD generators.

		open cycle	closed cycle
Anode parameters:			
Radius	[m]	0.11	0.11
Channel height	[m]	0.035	0.023
Cathode parameters:			
Radius	[m]	0.37	0.32
Channel height	[m]	0.009	0.014
Enthalpy extraction	[%]	8.7	37.0
Thermal input power	[MW]	10	5

Coil design

The basic solutions for the coil arrangement around an MHD disk channel are discussed in ref. 3. For our purpose we selected the split-pair magnet system. The design parameters of the magnet are mainly determined by the sizes of the channel and the thickness of both the channel and cryostat insulation. Therefore the minimum inner radius and the distance between the split-pair coils are 0.3 and 0.4 m respectively. To attain the desired field in the active region of the MHD channel, the magnet is split into two sections: a coil of NbTi providing the background field and an insert coil of Nb_3Sn that will enhance the field in the MHD channel up to 9 T, see figure 3. A distance between both coils in the radial direction of 0.03 m is required for the clamping structure of the Nb_3Sn coil and the connections of the helium cooling tubes. The winding volume is determined by the outer radius of the NbTi part and the coil thickness. The distribution of the winding volumes among both sections will introduce an additional parameter. Due to the difference in the costs of the NbTi and Nb_3Sn conductors this parameter can have a large impact on the manufacturing costs of the magnet.

Manuscript received September 24, 1990.

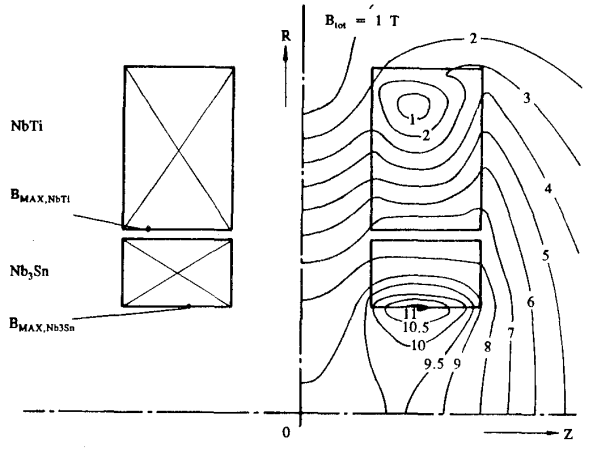

Figure 3. Magnetic field distribution in the coil sections and the surroundings of the split-pair magnet.

Coil optimization

The coil dimensions were optimized with respect to minimum conductor costs. Here a difference of a factor four between the costs per unit volume of the Nb_3Sn and NbTi conductors has been assumed. The optimization function includes both the design field in the MHD channel and the allowable field $B_{max,NbTi}$ at the inner turns of the outer coil section. A linear relationship between the overall current density and magnetic field in the NbTi coil has been assumed around a value of 47 A/mm^2 at 7 T. The overall current density in the insert coil is held constant at a conservative value of 30 A/mm^2. The change of the total conductor costs as function of the coil thickness is shown in figure 4. A minimum

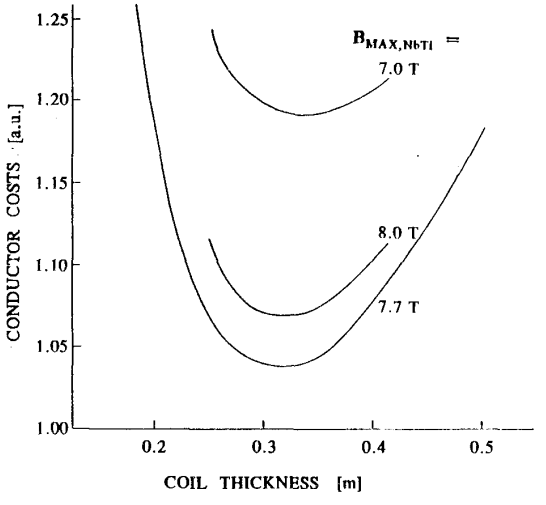

Figure 4. Conductor costs versus coil thickness.

in conductor costs is obtained with a coil thickness of 0.32 m. This value is almost independent of the maximum field in the NbTi windings. The minimum conductor costs change dramatically with $B_{max,NbTi}$ as indicated in figure 5. A sharp minimum appears at a value of 7.7 T at an overall current density of 37 A/mm^2. This minimum shifts to smaller $B_{max,NbTi}$ values if the difference in conductor costs between NbTi and Nb_3Sn reduces. The maximum field in the windings of the insert coil is also included in figure 5. A value of 11.1 T at a $B_{max,NbTi}$ of 7.7 T is determined and a small decay with increasing $B_{max,NbTi}$ can be noticed.

Conductor design

The concept of internally cooled Nb_3Sn and NbTi conductors has been adopted. Furthermore, the react-and-wind methode is

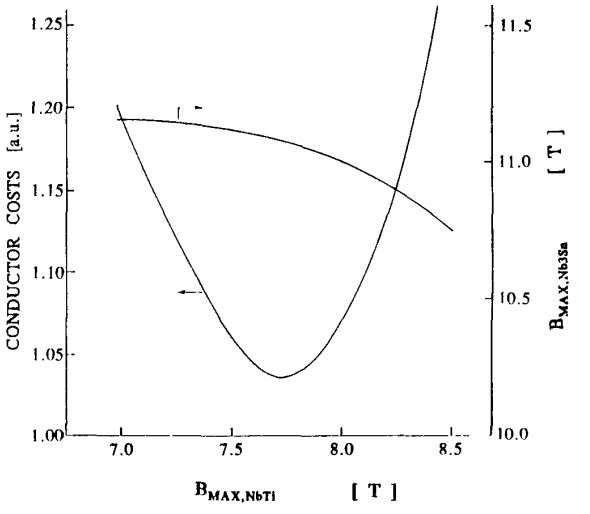

Figure 5. Conductor costs versus maximum field in the NbTi coil.

foreseen in manufacturing the Nb_3Sn sections. Due to this technique bending strain is introduced. To limit this strain, the Nb_3Sn layer in the composite conductor have to be located at the neutral axis of the conductor and its thickness must be as small as possible. Therefore the tube-cooled conductor in combination with a Rutherford cable is the best solution. A good behaviour of these composite conductors is obtained if the cross section has two right-angled symmetry axes so that tension builds up symmetrically[4].

The design values of the overall current density are rather conservative in order to achieve reliable magnet operation. Starting from the winding cross-section of the Nb_3Sn section of 0.32 x 0.194 m^2 and an operating current of 6.13 kA, the deduced dimensions of the composite conductor are 26.7 x 7.5 mm^2. The distribution of the available space among the constituents of the conductor, as listed in table 2, is determined by the current carrying capacity, the cryogenic stability and the maximum allowable stress in the materials used.

Table 2. Distribution of composite conductor constituents.

Composite conductor		Nb_3Sn	NbTi
cross section	[mm^2]	200	165
strand material	[mm^2]	22	25
stability material	[mm^2]	86	85
stainless steel reinforcement	[mm^2]	50	-
coolant	[mm^2]	20	25
insulation	[mm^2]	17	15
solder	[mm^2]	5	15

The mentioned overall current density in the Nb_3Sn section causes a hoop stress in the additional stabilization material of hard copper not more then 2/3 of its tensile yield strength.

Multifilamentary Nb_3Sn wires of 1.0 mm diameter produced by the "ECN powder technique" [5] show an exceptionally high current density. Using this conductor the thickness of the cable can be limited to 1.8 mm. Application of 28 strands results in a maximum critical current of 13 kA at 4.2 K and 11 T, if no degradation of current carrying capacity occurs. Furthermore, as result of the manufacturing process, the stability of this wire is better than those produced by the bronze process, due to the absence of the bronze among the filaments.

The layout of the proposed Nb_3Sn conductor is shown in figure 6a. The cable and the copper stabilization parts are soldered together and encapsulated by a stainless steel conduit with a thickness of 0.8 mm. In order to preserve symmetry the coolant surface is distributed over two channels of 5.3 x 1.8 mm^2 each and they are located at both thin edges of the sc. cable.

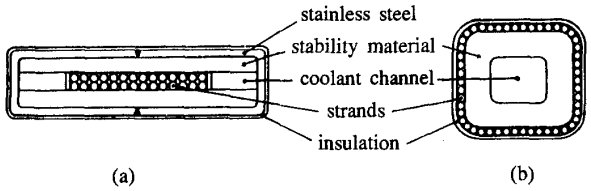

Figure 6. Layout of the Nb_3Sn (a) and NbTi (b) conductors. The dimensions are 26.7x7.5 mm^2 and 13.3x12.4 mm^2 respectively.

Figure 6b shows the internal layout of the proposed NbTi conductor. A conduit of cold worked copper with a wall thickness of 3.7 mm, creating a helium channel of 5.7 x 4.8 mm^2, also provides for stabilization and reinforcement. With the given conductor layout, the stress in the stabilization material will not exceed the maximum allowable value assuming no support of the outer windings. Thus additional reinforcement material is not necessary. Application of 50 NbTi/Cu strands with a diameter of 0.85 mm in the composite conductor, leads to a critical current of 10 kA at 7.7 T and an operating temperature of 4.5 K. The strands are twisted and soldered to the outer surface of the copper conduit.

Coil construction

To generate a field of 9 T in the centre of the MHD channel, the optimized Nb_3Sn and NbTi coil sections need $3.8 \cdot 10^6$ and $10.6 \cdot 10^6$ ampere-turns respectively. Coil dimensions and supplementary parameters of the split-pair magnet, defined at the nominal current of 6.13 kA are collected in table 3. Both conductors have their operating point substantially below the critical current, thus reliable long term operation can be expected.

Using forced flow cooling, it is advantageous to apply the double pancake winding technique. With this method the coil is build up from relative small modules that can be handled easily.

Table 3. Parameters of the magnet system for the disk facility.

Section		Nb_3Sn	NbTi
Winding inner radius	[m]	0.300	0.524
Winding outer radius	[m]	0.494	0.972
Coil thickness	[m]	0.320	0.320
Number of turns per coil		312	864
Conductor length per coil	[m]	786	4062
Mean current density	[A/mm^2]	31	37
Maximum field	[T]	11.1	7.7
Operating current	[kA]	6.13	6.13
Self inductance of each pair	[H]	1.45	
Self inductance coil system	[H]	3.64	
Stored energy total magnet	[MJ]	68.5	
Total joint resistance per coil section	[nΩ]	7	13
Number of double pancakes		12	24
Number of layers		26	36
Mass of bare magnet	[10^3 kg]	11	
Cold mass	[10^3 kg]	13	

Support struts

The cold mass, which consists of the coils, a containment structure to absorbe the attracting body force between both coils and a circular helium dewar, will be supported by six struts. These struts are constructed according to the approved methode of two concentric cylinders of G-10 fiber glass epoxy interconnected by a third cylinder of stainless steel, as shown in figure 7. The G-10 cylinders are connected between the temperature intervals 300-80 K and 80-4.5 K. They are exposed to compressive stress only. A N_2-radiation shield is connected to the stainless steel cylinder. In order to minimize the heat conduction through the G-10 material, the position of this shield in the strut was optimized. A ratio of 0.45 is found for the lengths of the G-10 cylinders, which have thicknesses of 5 mm.

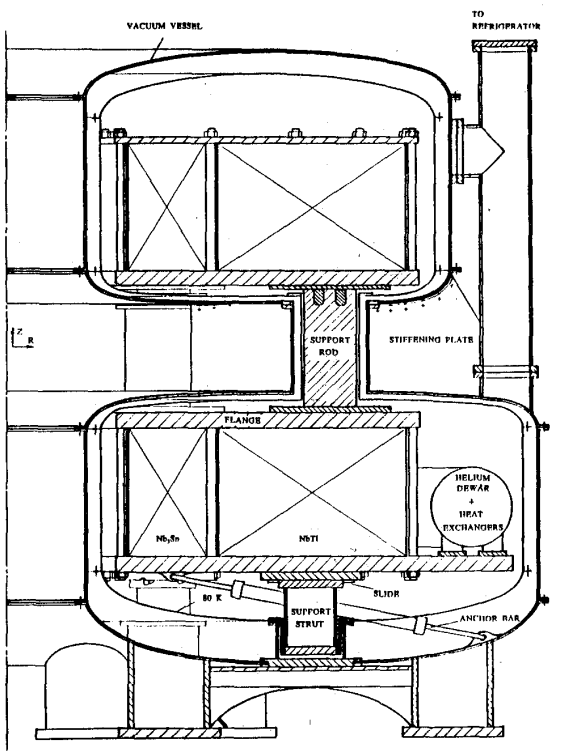

Figure 7. The cold mass in the vacuum vessel (cross sect. view).

Steady-state heat load

The cold mass, surrounded by the thermal shield in order to intercept conducted and radiated heat coming from the MHD channel, the walls of the vessel and the supporting struts, will be located in a vacuum vessel as shown in figure 7. The heat load of 180 W estimated for the thermal shield at 80 K is compensated by a liquid nitrogen flow of 0.9 g/s.

The magnet will be energized via current leads. The minimum heat load at the cold terminal of commercially available counter flow current leads is about 1 W/kA thus leading to a heat load of 12 W minimum. These leads have to be cooled by a helium gas flow rate of 0.3 g/s.

The steady state thermal loads for the cold mass are collected in table 4. The contribution of the lead loss to the total heat load is considerable. In order to limit these, it is desirable to connect the coil sections in series. The leads are connected to the NbTi-section. The heat flux into the helium from the NbTi and Nb_3Sn sections are approximately 90 and 60 mW/m^2 respectively. The total estimated dissipation can be met with a cooling power of 20 W at 4.5 K.

Table 4. Sources of cryogenic loss at 4.5 K.

Current leads	12.0 [W]
Radiation from LN2-shield	1.3 [W]
Joints	1.4 [W]
G-10 supporting struts	1.4 [W]
Others	2.0 [W]
Total loss at 4.5 K	18.1 [W]

Cooling technique

Supercritical helium circulates through the coils and heat exchangers. The latter ones, used to recool the helium, are positioned in the circular dewar which contains liquid helium at 4.5 K. A helium flow from the upper coils to the heat exchangers

is obtained by a cryogenic transfer line connected to both parts of the vacuum vessel. Downstream, the helium will expand in a Joule-Thomson valve and liquid and vaporized helium return to the circular helium dewar.

Both conductors include hydraulically smooth tubes. With a mass flow rate of the supercritical helium through the Nb_3Sn and NbTi section of 2.0 and 4.7 g/s respectively, the pressure drop is 0.30 kPa per meter of channel for both sections, calculated using the theory of ref. 6.

NbTi-section. When connecting 6 double pancakes hydraulically in series, the total pressure drop will be 0.6 MPa. A total of 4 parallel cooling channels in both NbTi sections are foreseen. Each channel starts at the plane of symmetry at the outer radius of a section. The inlet pressure is 1.5 MPa at a temperature of 4.5 K.

In order to limit the dissipation in the coils, the temperature should not exceed the current sharing temperature of 4.86 K. This means that interim cooling has to take place after passing two double pancakes. Before entering into the heat exchangers, both channels of a section are joined together.

Nb_3Sn-section. All pancakes of the Nb_3Sn section are connected hydraulically in series. The conductor length is 1570 m and the pressure drop is 0.47 MPa. Interim cooling of the helium to 4.5 K takes place three times. Supercritical helium of 4.5 K will enter at the midplane of the section. Inlet and outlet connections are located at the outer radius of the coil section.

Stability and current margin

The cryogenic stability parameter α as formulated by the Stekly criterion is determined by application of the Dittus - Boelter turbulent heat transfer correlation[6]. With the assumed

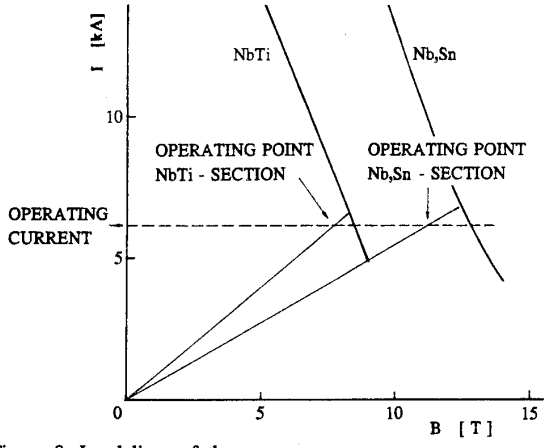

Figure 8. Load lines of the magnet.

mass flow rate and the resistivity for cold work copper used in the NbTi and Nb_3Sn conductor of 5.6 and $9.4 \cdot 10^{-10}$ Ωm, values of 4.8 and 1.9 for the NbTi and Nb_3Sn coils are found. Especially the α-parameter for NbTi indicates a substantial deviation from cryogenic stability. However, many medium size magnets can work far below the level of full cryostability of $\alpha = 1$.

Figure 8 shows the load lines of the magnet. The I_c data of NbTi and Nb_3Sn are based on 2000 A/mm^2 at 5 T and 2000 A/mm^2 at 10 T respectively. When the magnet is energized, the ratios of the nominal current to the critical current for the NbTi section and Nb_3Sn section are 0.72 and 0.62. A degradation of the critical current of 20 % due to stress effects and cable manufacturing is assumed for both conductors.

Magnetic field distribution

The decay of the axial field component B_z in the radial direction, when both sections are energized, is shown in figure 9. In the centre of the MHD channel this field is 9.05 T. At the anode of the disk generator this field is 9.0 T and will decrease to about 7 T at the position of the cathode. The maximum radial field component that will occur in this part of the MHD channel, is limited to 0.2 T. The field distribution due to the separate sections is also shown in figure 9.

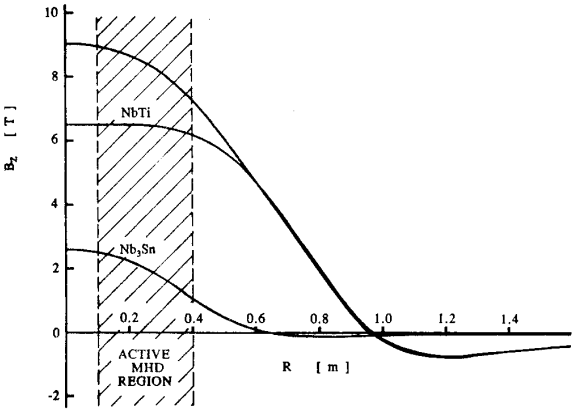

Figure 9. Field distribution as a function of radius in the centre of the MHD channel.

Conclusions

To obtain the desired magnetic field of 9 T in the active area of the MHD channel, the magnet is split into a NbTi and a Nb_3Sn section. Optimization with respect to minimum conductor costs has been worked out.

Cooling of the magnet at 4 K is provided by forced flow supercritical helium.

Full cryogenic stability is not pursued. Stekly parameters of 4.8 and 1.9 for the NbTi and Nb_3Sn sections are obtained.

The size of the facility of 10 MWt is small enough to limit the investment costs and large enough to gain insight in the physics of MHD disk generators.

The proposed experimental facility will serve the need for extension of the knowledge on the behaviour of MHD disk generators.

Acknowledgement

These investigations in the programme of the Foundation for Fundamental Research on Matter FOM have been supported in part by the Netherlands Technology Foundation STW, Utrecht, The Netherlands.

References

1. P. Massee, H.A.L.M de Graaf, W.J.M. Balemans, H.G. Knoopers and H.H.J. ten Kate, "System studies of closed and open cycle disk and linear MHD generators", *10th Intern. Conf. on MHD Electr. Power Generation*, Tiruchirapalli, Vol II, X31-X38, 1989.

2. P. Massee, H.G. Knoopers, H.H.J. ten Kate, H.A.L.M de Graaf and W.J.M. Balemans. "Predesign of an experimental (5-10 MWt) disk MHD facility and prospects of commercial (1000 MWt) MHD/steam systems", University of Twente, ISBN 90-365-0317-5.

3. H.G. Knoopers, H.H.J. ten Kate, L.J.M. van de Klundert, P. Massee, H.A.L.M de Graaf and W.J.M. Balemans. "Superconducting magnets for disk-shaped MHD generators:review and predesign", *Proc. MT-11*, Tsukuba, Japan, 513-518, 1989.

4. J.J. Alff, "Strain problems associated with the winding of reacted Nb_3Sn superconductors", *Proc. MT-9* Zurich,669-672,1985.

5. H.H.J. ten Kate, B. ten Haken, S. Wessel, J.A. Eikelboom and E.M. Hornsveld. "Critical current measurements of prototype cables for the CERN LHC up to 50 kA and between 7 and 13 Tesla using a superconducting transformer circuit", *Proc. MT-11*, Tsukuba, Japan, 60-65, 1989.

6. Van Sciver, S.W., "Helium Cryogenics", Plenum Press, New York (1986).